

Modeling the Effect of Void Shapes on the Compressive Behavior of Parallel-Strand Lumber

Alireza Amini¹; Sanjay R. Arwade²; and Peggi L. Clouston, M.ASCE³

Abstract: Small voids of varying shapes and sizes are an inherent part of the physical structure of parallel strand lumber (PSL) due to the material's manufacturing process. To gauge the sensitivity of the material's mechanical behavior to these voids, this paper proposes and evaluates finite element models that incorporate PSL voids by simulating them as equivalent ellipsoids. It is assumed that the wood phase is a homogeneous and orthotropic continuum, while the void phase is the only source of uncertainty. Two analyses are presented: (1) linear elastic analyses to gauge the effective modulus of elasticity and the distribution of conventional, principal, and effective stresses considering the effect of volume fraction and void shape; (2) nonlinear analyses under uniaxial and biaxial ductile compressive loading scenarios. Linear elastic analyses showed that representing voids as equivalent ellipsoids does not affect the effective elastic moduli and stress distributions in the models under uniaxial loading. Nonlinear analyses confirmed that the overall nonlinear compressive behavior of the models with equivalent ellipsoids are similar to that of their corresponding models with actual voids. DOI: 10.1061/(ASCE)MT.1943-5533.0001980. © 2017 American Society of Civil Engineers.

Author keywords: Parallel strand lumber; Heterogeneous and orthotropic material; Mesostructure; Void shape effect; Ductile and brittle behavior.

Introduction

Parallel strand lumber (PSL) is a common engineered wood product used primarily as beams and columns in the North American construction sector. It is composed of parallel wood strands compacted and glued together with a proprietary phenol-resorcinol adhesive. Its strength is well-known to be more reliable than that of traditional solid sawn lumber as a result of the reduction and dispersion of wood knots and defects in the process of manufacturing. Consequently, PSL has gained popularity over past decades as a replacement for conventional lumber in residential applications as well as becoming direct competition for steel and concrete in commercial and industrial applications.

PSL is made from long strands of wood veneer that are first roughly oriented in the longitudinal direction before being glue-laminated into large rectangular billets. The inexact nature of the manufacturing process leads to a physical material structure that, at a mesoscale (the scale of average strand width; i.e., millimeters scale), contains voids of varying shapes and sizes (Fig. 1). In a previous study (Amini et al. 2014), the authors developed a statistical characterization of this void field approximating naturally occurring voids as ellipsoids.

Modeling the effect of wood composite mesostructure on mechanical behavior has been a topic of interest to researchers for years. In one of the first attempts to model PSL, a nonlinear stochastic model was formulated by Clouston and Lam (2001), who successfully simulated the stress-strain behavior of strand-based wood composites based on orthotropic and spatially variable constitutive properties of wood strands using probabilistic plasticity theory and the Tsai-Wu yield surface. Further to this work, a model for spatial variation of the elastic modulus of PSL was developed by Arwade et al. (2009). This work included a stochastic computational model that incorporated orthotropic elasticity and uncertainty in strand geometry and material properties. The same authors also investigated the variability of compressive strength of PSL by conducting the measurement of compressive strength on specimens of varying size (Arwade et al. 2010) and developed a computational model which included the strand length, grain angle, elastic constants, and parameters of Tsai-Hill failure surface. Bejo and Lang (2004) also proposed a probability-based model to study the effect of the change in elastic properties on the performance of the product and modeled the orthotropic behavior of wood constituents as a result of their position in the composite employing theoretical and empirical equations.

While these previous studies significantly advanced the methodology and the accuracy of wood composite strength modeling, no study incorporated the presence of voids in the mesostructure. In this study, the mesostructure of PSL is first modeled based on the methodology outlined in the previous paper by the same authors (Amini et al. 2014). This previous work measured the void phase of PSL through serial sectioning to produce two-dimensional (2D) and three-dimensional (3D) distributions of the void structure. Equivalent ellipsoids were fitted to actual void shapes. Ellipsoids were the chosen shape because they are relatively easy and computationally efficient to model given that they have well-known and definable geometric parameters.

The objective of this paper is, therefore, to test the hypothesis that the virtual ellipsoidal voids defined in (Amini et al. 2014) are appropriate replacements for the actual voids in strength modeling.

¹Senior Structural Engineer, Prime AE Group, 2nd Floor, 55 Capital Blvd., Rocky Hill, CT 06067; formerly, Graduate Student, Dept. of Civil and Environmental Engineering, Univ. of Massachusetts at Amherst, Amherst, MA 01003 (corresponding author). E-mail: ar.amini@gmail.com

²Professor, Dept. of Civil and Environmental Engineering, Univ. of Massachusetts at Amherst, Amherst, MA 01003.

³Associate Professor, Dept. of Environmental Conservation, Univ. of Massachusetts at Amherst, Amherst, MA 01003.

Note. This manuscript was submitted on August 4, 2016; approved on February 13, 2017; published online on May 16, 2017. Discussion period open until October 16, 2017; separate discussions must be submitted for individual papers. This paper is part of the *Journal of Materials in Civil Engineering*, © ASCE, ISSN 0899-1561.

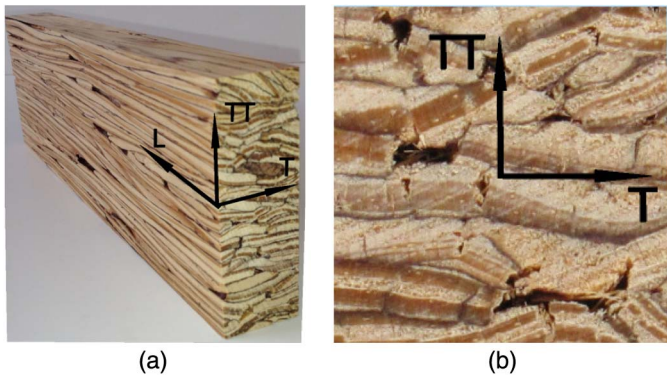


Fig. 1. Cross-sectional views of PSL specimen and definition of the member coordinate system (dark spots are voids; L = longitudinal, T = transverse, TT = thru thickness): (a) 3D view; (b) T-TT section

It is understood that approximating randomly shaped actual voids (that could have sharp tips, for example) as smooth ellipsoids may affect the predicted stress distribution. The finite element model may not detect appropriate stress concentration at the tip of an ellipsoidal void. Also, the void tips may cause local multiaxiality (i.e., the existence of large stresses in the directions other than the direction of loading). The statistical void characterization presented in Amini et al. (2014) will be implemented into finite element models to predict the effect of void shapes on the mechanical behavior of PSL under compressive loading conditions.

Parallel strand lumber is known to exhibit different mechanical behavior under compression (ductile) and tension (brittle). This study considers linear elastic analyses and nonlinear plastic analyses considering both uniaxial and biaxial compression loading scenarios.

Background

Fig. 1 depicts the orthotropic mesostructure of PSL which consists of wood strands, adhesive, and voids. The physical and mechanical variability in the strands, along with the voids, result in material heterogeneity. The coordinate system is defined by the axes L, T, and TT, which represent longitudinal, transverse, and through thickness directions of PSL, respectively.

It was shown in a previous study (Amini et al. 2014) that the ellipsoidal shape is a good approximation for the actual void shape

in so much as the volumes, moments of inertia, and the aspect ratios of moments of inertia of equivalent ellipsoids match well to that of actual voids. In this previous study, the mean ellipsoid dimensions R_1 , R_2 , and R_3 were calibrated to the actual void statistics to match at least the second moment properties of the actual void shapes. Fig. 2(a) illustrates a T-TT section of PSL where 2D voids are replaced with equivalent ellipses. In Fig. 2(b), an equivalent ellipsoid is fitted to a three-voxel void.

Linear Elastic Analysis

As a first step of this work, linear elastic analyses were conducted to gauge whether actual voids could be replaced with equivalent ellipsoids without compromising numerical accuracy of effective modulus. Two sets of finite element models were created of uniaxial compressive loadings along the three main material directions: one set using a 3D specimen with carefully measured actual voids, and one set whereby the actual voids were replaced with corresponding equivalent ellipsoids. Fig. 3(a) displays schematically the dimensions, loading and boundary conditions of the models. Tables 1 and 3 outline the material properties of 2.0E SP PSL material (PSL material made of Southern pine species with 2.0×10^6 psi elastic modulus) used in this study. The properties were taken from (or calculated based on the provisions of) the previous studies Woodhandbook (Forest Products Laboratory 2010), Janowiak et al. (2000), and Jones (1975). The details of the analysis are provided in Amini (2013) and are not included in this paper for sake of brevity. The analyses compared (1) effective elastic constants, (2) stress concentrations, and (3) local multiaxiality differences under compressive loading for all three orthogonal directions.

The replacement of ellipsoids does not cause a considerable change in the effective elastic modulus, especially along L direction, which is the largest and usually the most important to engineering design. The important statistical properties of the element normalized stresses [calculated by Eq. (1)] in both actual and equivalent models have been presented in Table 2. In all six simulations, the means and medians of all types of stresses almost match with less than 1% difference for loading in L and TT directions and less than 10% difference for loading in T direction. For loading in TT and L directions, the standard deviations of all types of stresses in actual models are larger than that of the equivalent models. This is the effect of the sharp void tips in actual models compared to

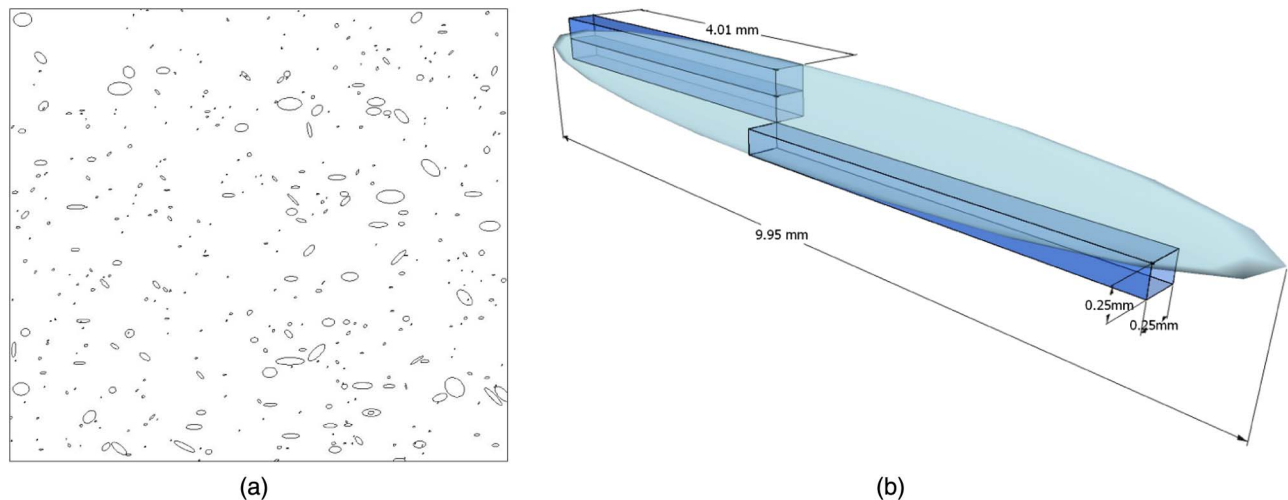


Fig. 2. 2D illustration of void replacements and a scheme of 3D replacement: (a) ellipses replaced 2D voids; (b) ellipsoid fitted to a 3-voxel void

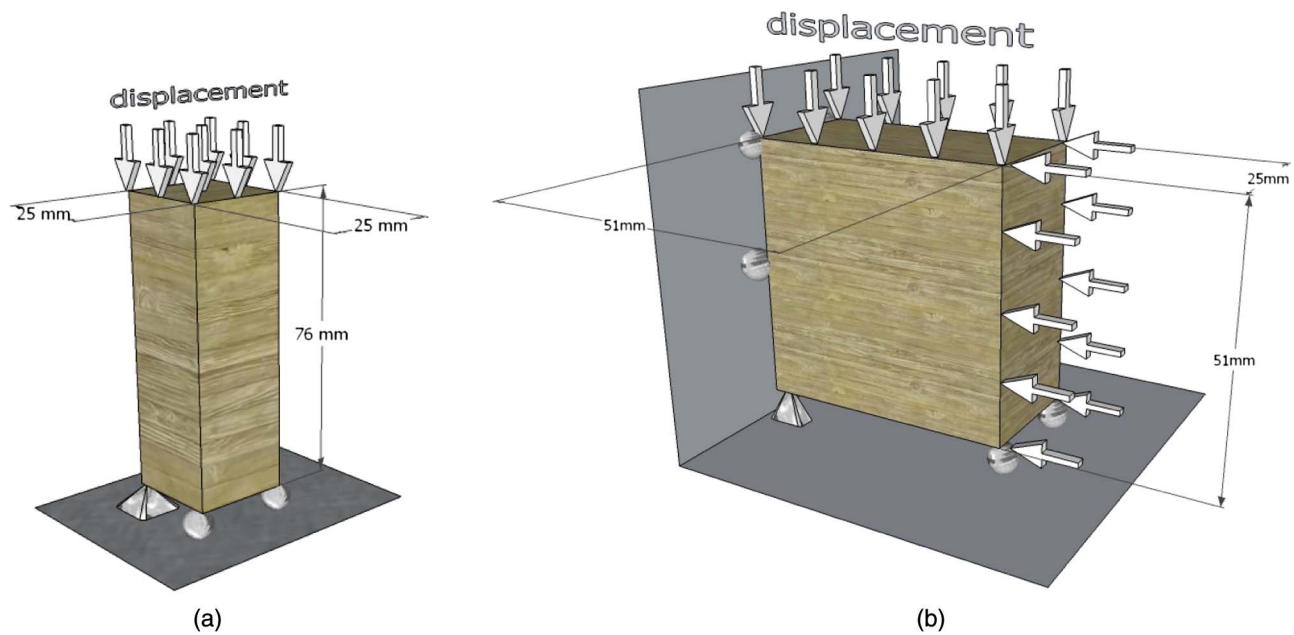


Fig. 3. Schematic sketch of finite element models of PSL: (a) uniaxial linear and nonlinear analyses; (b) biaxial nonlinear compressive analyses

Table 1. Elastic Constants of PSL Strands (E_x : Elastic Modulus in x Direction, ν_{xy} : Poisson's Ratio in x and y Directions, G_{xy} : Shear Modulus in x and y Directions)

Material property	Value
E_L (MPa)	13,000
E_T (MPa)	650
E_{TT} (MPa)	650
ν_{TL}	0.15
ν_{TTL}	0.15
ν_{TTT}	0.09
G_{TL} (MPa)	500
G_{TTL} (MPa)	400
G_{TTT} (MPa)	85

Table 2. Statistics of the Normalized Element Stresses (with Zero Mean) When Actual and Equivalent Models Have Been Loaded in Different Material Directions ($\sigma_{x,N}$: Normalized Normal Stress in x Direction, $\sigma_{3,N}$: Normalized Maximum Principal Stress)

Measure	Model type	Loading in L		Loading in T		Loading in TT	
		$\sigma_{L,N}$	$\sigma_{3,N}$	$\sigma_{T,N}$	$\sigma_{3,N}$	$\sigma_{TT,N}$	$\sigma_{3,N}$
Median	Actual	0	0	0.01	0	0.01	0
	Equivalent	0	0	0.03	0.02	0.02	0.01
Standard deviation	Actual	0.06	0.06	0.14	0.13	0.29	0.27
	Equivalent	0.04	0.04	0.30	0.29	0.24	0.23

the smooth tips of equivalent ellipsoids. Also, no influential stress multiaxiality state has been detected in any of actual and equivalent void models under any defined loading scenario

$$\sigma_{i,N} = \frac{\sigma_i}{\text{mean}(\sigma_i)} - 1 \quad (1)$$

where i = direction of stress (i.e., T, TT, L, or 3 for the maximum principal stress).

Table 3. Strength Values of PSL Strands in Different Material Directions (S_x : Strength in x Direction)

Strength	Value (MPa)
S_T in compression	6.2
S_T in tension	1.5
S_{TT} in compression	6.2
S_{TT} in tension	1.5
S_L in compression	53.5
S_L in tension	53.7
S_{TTT}	9.2
S_{TL}	5.9
S_{TTL}	9.2

Nonlinear Compressive Analysis

Finite Element Formulation

A total of 60 separate finite element models were created and analyzed for compressive loading; that is, five different geometries (i.e., replications) were created for both actual void specimens and corresponding ellipsoidal void specimens. Further, loading was applied in each of the three material directions for both uniaxial loading and biaxial loading (i.e., 5 5 replications \times 2 void shape models \times 3 material directions \times 2 load cases = 60 separate models). Multiple geometries were considered for each void model to investigate the effect that void size, location, and distribution may have on the local magnitude of stresses, potentially driving the model into nonlinear behavior either locally or globally. Each actual void model was picked from a random location in a 133 \times 133 \times 610 mm PSL billet, which had been characterized for this project (Amini et al. 2014). After the analysis of actual void model, the voids were replaced by their equivalent ellipsoids, and the analysis was repeated.

To define the terminology which will be used in this section, the scheme of the expected constitutive behavior of PSL material under compression is illustrated in Fig. 4(a). This scheme is based on the hypothesis that PSL's constitutive behavior should not be very different from that of solid-sawn lumber. The symbols σ_c and ε_c

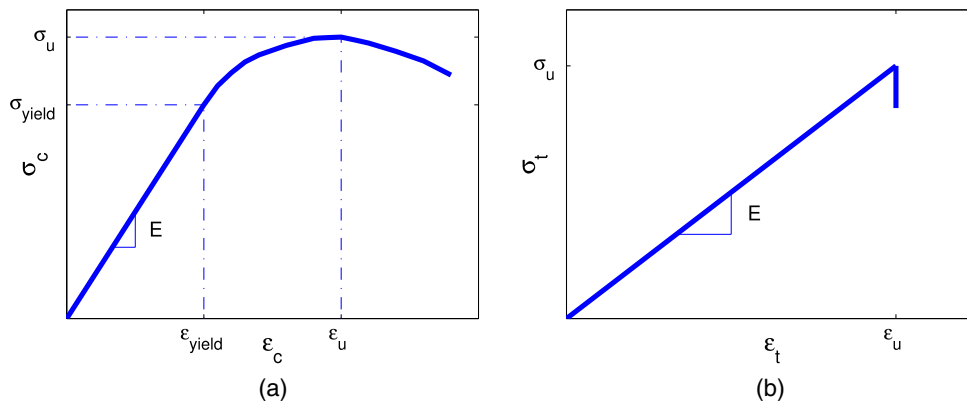


Fig. 4. Schemes of the expected stress-strain relationship of PSL: (a) under compression; (b) under tension

represent compressive stress and compressive strain respectively. As shown in this figure, σ_{yield} and $\varepsilon_{\text{yield}}$ are respectively the compressive stress and strain at which the material yields (switches from linear elastic phase with elastic modulus E to nonlinear plastic phase with varying plastic modulus). They are called *compressive yield stress* and *compressive yield strain* (since no yielding behavior is expected under tensile loading, they are simply called yield stress and yield strain). The maximum compressive stress which the material bears is called *compressive strength* or *compressive ultimate stress* and labeled by σ_u . The strain corresponding to the compressive ultimate stress is called *compressive ultimate strain* (ε_u). Note that this strain may be less than the maximum strain that the material experiences.

For uniaxial loading [Fig. 3(a)], the specimen dimensions were $25 \times 25 \times 76$ mm. The model's longest side was always in the direction of loading. These dimensions were selected to match the size of the specimens tested by Arwade et al. (2010) to ease the future comparison of experimental and numerical results. The finite element models assumed displacement control with the total displacement of 1 mm (total strain of 1.3%) for the loading in T or TT direction and 0.6 mm total displacement (0.8% total strain) for the loading in L direction.

For biaxial loading [Fig. 3(b)], the specimen dimensions were $25 \times 51 \times 51$ mm. The two 51-mm dimensions were oriented along the two loading directions. In the case of loading along T or TT directions, the total applied displacement was 0.7 mm (1.4% total strain), and the applied total displacement in L direction was 0.4 mm (0.8% total strain). The reason for this difference was that the elastic modulus in L direction is much larger than that of T and TT directions, and, therefore, a small strain in L direction could cause a large stress. Also, uniaxial simulations and Winans' tests (Arwade et al. 2010) showed that the yield and ultimate strains of PSL in the L direction are smaller than that of other two directions. In all simulations, the displacements were applied in 15 steps, in a way that the first step was large enough to cover most of the linear-elastic deformation, and the other 14 steps were equally small to track the nonlinear deformation.

The size of each 3D solid finite element was the same as the digital voxels (Amini et al. 2014), $0.25 \times 0.25 \times 4.02$ mm in the T, TT, and L directions, respectively. A convergence test confirmed that the aspect ratio of the elements was acceptable for loadings in T and TT directions (Amini 2013).

Boundary conditions were applied at nodes at the base of each model. For all models, one base node was constrained for the three displacement directions, while the other base nodes were constrained along the direction of loading. The models consisted of two material phases: wood strands and voids. The wood strands

were assumed to behave elastic-perfectly plastic at the yield stress and orthotropic with properties per Tables 1 and 3. Compared to the known constitutive behavior of PSL under compression as illustrated in Fig. 4(a), the assumption of perfect plasticity is a simplification but was not expected to affect results substantially. Identical compressive strength values taken from Wood-handbook (Forest Products Laboratory 2010) were used as the strands' yield stress.

Hill's failure criterion has been selected to model wood's nonlinear compressive behavior at the time of failure. This failure criterion is given by reference (ADINA R&D 2012) as follows:

$$f_{\text{yield}} = F(\sigma_{bb} - \sigma_{cc})^2 + G(\sigma_{cc} - \sigma_{aa})^2 + H(\sigma_{aa} - \sigma_{bb})^2 + 2L\sigma_{ab}^2 + 2M\sigma_{bc}^2 + 2N\sigma_{ac}^2 - 1 = 0 \quad (2)$$

where (a, b, c) = material principal axes, and F, G, H, L, M, N = material constants given by

$$F = \frac{1}{2} \left(\frac{1}{Y_{bb}^2} + \frac{1}{Y_{cc}^2} - \frac{1}{Y_{aa}^2} \right) \quad (3)$$

$$G = \frac{1}{2} \left(\frac{1}{Y_{cc}^2} + \frac{1}{Y_{aa}^2} - \frac{1}{Y_{bb}^2} \right) \quad (4)$$

$$H = \frac{1}{2} \left(\frac{1}{Y_{aa}^2} + \frac{1}{Y_{bb}^2} - \frac{1}{Y_{cc}^2} \right) \quad (5)$$

$$L = \frac{1}{2Y_{ab}^2} \quad (6)$$

$$M = \frac{1}{2Y_{bc}^2} \quad (7)$$

$$N = \frac{1}{2Y_{ac}^2} \quad (8)$$

where Y_{aa}, Y_{bb}, Y_{cc} = yield stresses in the material directions a, b, c and Y_{ab}, Y_{ac}, Y_{bc} = yield stresses for pure shear in the planes $(a, b), (a, c),$ and (b, c) . f_{yield} = dimensionless. In SI, the units of F, G, H, L, M and N are all $1/\text{MPa}^2$.

Compression Analyses Results

Uniaxial Loading

Fig. 5 illustrates the mechanical behavior of actual versus ellipsoidal void models for loading in the three material directions, and

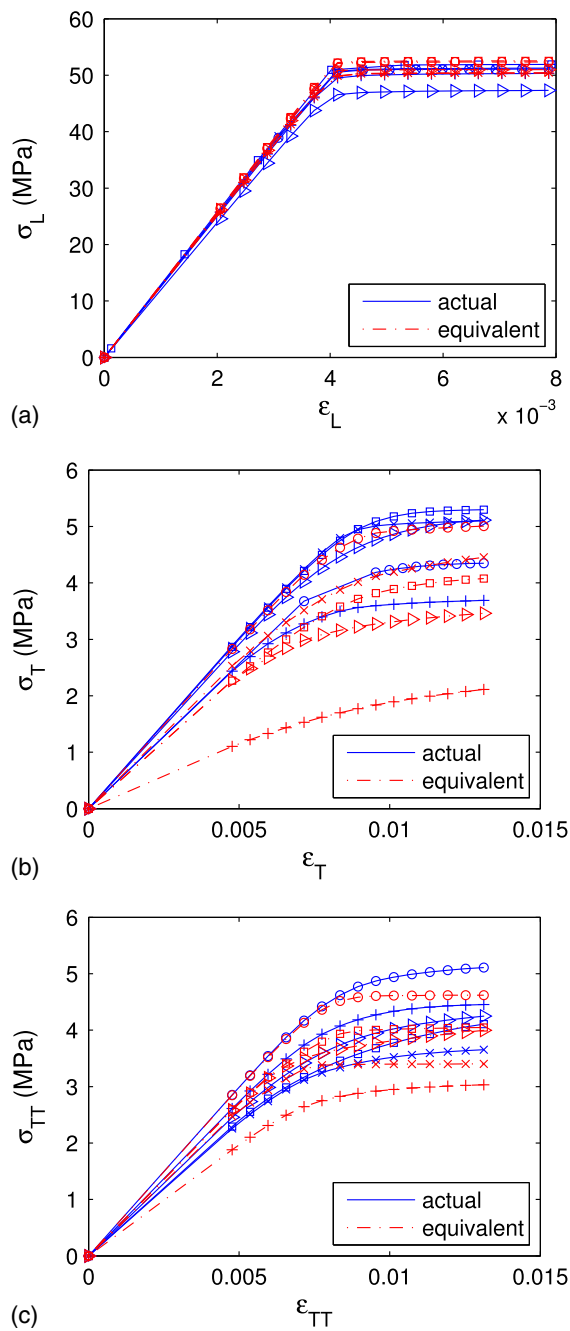


Fig. 5. Comparison of normal stresses along the direction of loading in the corresponding actual and equivalent models under uniaxial compressive loading in each material direction (σ_x : normal stress in x direction; ϵ_x : normal strain in x direction): (a) loading in L direction; (b) loading in T direction; (c) loading in TT direction

Table 4 lists the corresponding mean and standard deviation values for yield stress, ultimate stress, and strain to compare both void models and loading directions.

For loading in the L direction, the behavior is almost elastic perfectly-plastic, and the two void models are in good agreement. The mean and standard deviation of the longitudinal strength (i.e., ultimate stress) for actual models are 50.4 and 1.8 MPa, respectively, while the corresponding values for equivalent models are 51.3 and 1.0 MPa. Yield stresses [calculated using the 0.2% offset yield strain method (Hibbeler 2011)] has mean and standard deviation values of 49.6 and 1.8 MPa (actual) versus 51.0 and

1.1 MPa (ellipsoidal). The difference between mean ultimate and yield stress values is 1.8 and 2.8%, respectively.

The standard deviation of stresses in actual models are more than that in equivalent models, which is expected considering the fact that there is more variation in the arbitrary shape of the actual voids compared to the smooth shape of the ellipsoids.

As for loading in the T and TT directions, slightly larger differences were found between the strength and yield stress of the two void models. The values for the actual void models were, on average, larger than that of the ellipsoidal void models, which is contrary to the expectation that the smooth shape of ellipsoids would lead to lower stress concentrations and consequently higher total strength.

Loading in T direction, there was approximately 19 and 22% difference between mean strength and yield stress, while loading in TT direction, there was approximately 12 and 10% difference between mean strength and yield stress comparing the two void models.

A possible reason for such differences between actual and ellipsoidal void models loaded in T and TT directions is that, in some cases, the method of fitting ellipsoids to the actual voids explained in Amini et al. (2014) changes the aspect ratio of voids in the T-TT plane. Since the main objective of the mentioned method is to generate an ellipsoid with similar volume and length to the actual void, the distortion of aspect ratio in T-TT plane is possible. The statistical tests explained in the next section show that the ellipsoids are still good replacements for the actual voids even when the loading is along the T or TT direction.

Statistical Testing

The Student's T-test and Wilcoxon signed rank test (Mc Clave 2012) were conducted to evaluate whether replacing actual voids in a PSL specimen by equivalent ellipsoids significantly altered the material's predicted ductile behavior under uniaxial compressive loading along each material direction. Specifically, the null hypothesis (H_{0p}) is that the distributions of the yield and ultimate stresses of the corresponding sets of actual and equivalent models are equivalent. The Student's T-test performs a paired test of the null hypothesis that the difference $x_a - x_e$ is a random sample from a normal distribution with mean zero and unknown variance, against the alternative that the mean is not zero. Here, x_a and x_e are the arrays containing the values of yield (or ultimate) stresses of the corresponding actual and equivalent models, respectively. Wilcoxon test performs a paired, two-sided signed rank test of the null hypothesis that data in the array $x_a - x_e$ come from a continuous, symmetric distribution with zero median, against the alternative that the distribution does not have zero median. The hypothesis of zero median for $x_a - x_e$ is not necessarily equivalent to the hypothesis of equal median for x_a and x_e . In this study, because it is not known whether the distribution of $x_a - x_e$ is normal or not, both the Student's T (parametric) and Wilcoxon (nonparametric) tests are employed to arrive at a more inclusive conclusion.

The p-value of a T or a Wilcoxon test is the probability, under the null hypothesis, of observing a value as extreme or more extreme of the test (in our case: simulation) statistics. The bigger the p-value, the higher the probability that the two arrays are the samples taken from the same distribution. Usually, a p-value less 5% leads to the rejection of the null hypothesis.

Table 5 lists the p-values calculated by the Student's T and Wilcoxon tests. All the p-values are above 5%, indicating that the uniaxial simulations do not provide evidence to reject H_{0p} . Especially for loading in the L direction, the p-values are quite high, so there is a high level of confidence that distributions of the yield and ultimate stresses of the corresponding sets of actual and

Table 4. Mean and Standard Deviation of the Yield and Ultimate Stresses and Strains of the Corresponding Actual and Equivalent Models Taken from the Same Position in the Parent Billet under Uniaxial Compressive Loadings in Three Material Directions

Loading direction	T		TT		L	
	Actual	Equivalent	Actual	Equivalent	Actual	Equivalent
σ_{yield}						
Mean (MPa)	4.6	3.6	4.1	3.7	49.6	51.0
Standard deviation (MPa)	0.7	1.1	0.6	0.6	1.8	1.1
$\varepsilon_{\text{yield}}$						
Mean (%)	1.01	0.99	0.98	0.92	0.41	0.41
Standard deviation (%)	0.07	0.07	0.04	0.05	0	0
σ_u						
Mean (MPa)	4.7	3.8	4.3	3.8	50.4	51.3
Standard deviation (MPa)	0.7	1.1	0.5	0.6	1.8	1.0
ε_u						
Mean (%)	1.31	1.31	1.31	1.31	0.79	0.79
Standard deviation (%)	0	0	0	0	0	0

Table 5. p -Values of Student's T and Wilcoxon Tests under the Null Hypothesis H_{0p} Evaluated for the Uniaxial Loading Scenarios

Loading direction	Yield stress		Ultimate stress	
	T-test (%)	Wilcoxon test (%)	T-test (%)	Wilcoxon test (%)
T	9.0	15.1	10.5	15.1
TT	27.9	54.8	11.0	22.2
L	19.1	31.0	27.5	54.8

equivalent models are equivalent. An increase in the number of replications may change p -values, but it is unlikely that such high p -values would drop to under 5%.

Biaxial Loading

Fig. 6 and Table 6 present the biaxial compressive loading model results. When loaded along T + TT directions, there is 6% difference between the maximum stresses along the T direction comparing actual and ellipsoidal models and just about 1% difference between those along the TT direction. Loading in the T + L directions, the results are less reassuring, with the difference between the mean maximum stresses along the T direction being 20%. Along the TT + L directions, the difference amounts to 6 and 2% in the values of mean maximum stresses along TT and L directions respectively in the actual and ellipsoidal models.

Interestingly, softening behavior is predicted when models are loaded biaxially in T + L or TT + L directions [Figs. 6(a and c)]. In these two cases, the induced stresses in L direction are much larger than the stresses in the perpendicular directions. The cause of softening here is most likely due to the interaction of stresses (i.e., Poisson's effect), since the wood strand constitutive model is still considered elastic-perfectly-plastic, and no softening behavior was observed for the uniaxial simulations. Also, the Poisson's ratios in T-L and TT-L planes are rather large (0.15). Therefore, the longitudinal axial stress interacts with the axial stress in T or TT direction (based on the direction of loading) causes the reduction in the ultimate stress of PSL material in T or TT direction and ultimately results in softening.

Another interesting point is that although the strands yield stress in both T and TT directions is 6.2 MPa and the material models are elastic perfectly-plastic, stresses induced by the loading in T + TT directions reach 8 MPa and then tend to increase if more displacement is applied [Figs. 6(e and f)]. It seems that Poisson's effect here acts positively, and results in the strength increase.

A possible explanation why a biaxial state of stress (and Poisson's effect) may cause softening in the case of loading in T + L

and TT + L directions, but hardening in the case of loading in T + TT directions is as follows:

Considering Eq. (2) in which directions a, b, c are, respectively, X (or T), Y (or TT), Z (or L) directions, Y_{aa}, Y_{bb}, Y_{cc} are assumed equal to $S_X = 6.2$ MPa, $S_Y = 6.2$ MPa, $S_Z = 53.3$ MPa (Table 2). It is noted that in (Amini 2013), the stress multi-axiality is negligible if PSL is loaded uniaxially.

Here, multi-axiality is even less probable since the biaxial loading is present in the boundary conditions. Thus, under biaxial loading, all shearing stresses, as well as normal stresses in the unloaded direction, are zero. Loading in the T + L directions, f_{yield} becomes

$$f_{\text{yield}} = \frac{(\sigma_X^2 + \sigma_Z^2 - \sigma_X \sigma_Z)}{(53.5 \text{ MPa})^2} + \frac{(\sigma_X - \sigma_Z)^2}{(6.2 \text{ MPa})^2} - 1 \quad (9)$$

The first term in Eq. (9) is much smaller than the second term because it has a much larger denominator, so drop the first term and assume

$$f_{\text{yield}} = \frac{(\sigma_X - \sigma_Z)^2}{(6.2 \text{ MPa})^2} - 1 \quad (10)$$

With the same reasoning, if the model is loaded uniaxially in the T direction, the approximate Hill's yield function will be

$$f_{\text{yield}} = \frac{\sigma_X^2}{(6.2 \text{ MPa})^2} - 1 \quad (11)$$

Since E_L is 20 times E_T , the change in σ_Z ($\Delta\sigma_Z$) in each loading step is much larger than the change in σ_X ($\Delta\sigma_X$). Remember that this analysis is displacement control, and, in fact, in each loading step certain displacements are applied in the T and L directions. Also, the applied displacements in L direction are always smaller than those in the T direction but not 20 times smaller; they are about half of the displacement steps in the T direction. Hence

$$\Delta\sigma_Z \approx 10\Delta\sigma_X \Rightarrow \Delta(\sigma_Z - \sigma_X) > \Delta\sigma_X \quad (12)$$

One can conclude from Eqs. (10)–(12) that in the case of biaxial loading in the T + L directions, f_{yield} approaches zero much faster than it does in the case of uniaxial loading in the T direction. Therefore, comparing these two loading scenarios, the model's yield stress must be lower in T + L loading. Also, large values of $\Delta(\sigma_Z - \sigma_X)$ cause softening in the model.

On the other hand, under biaxial loading in the T + TT direction, the approximate Hill's yield function is

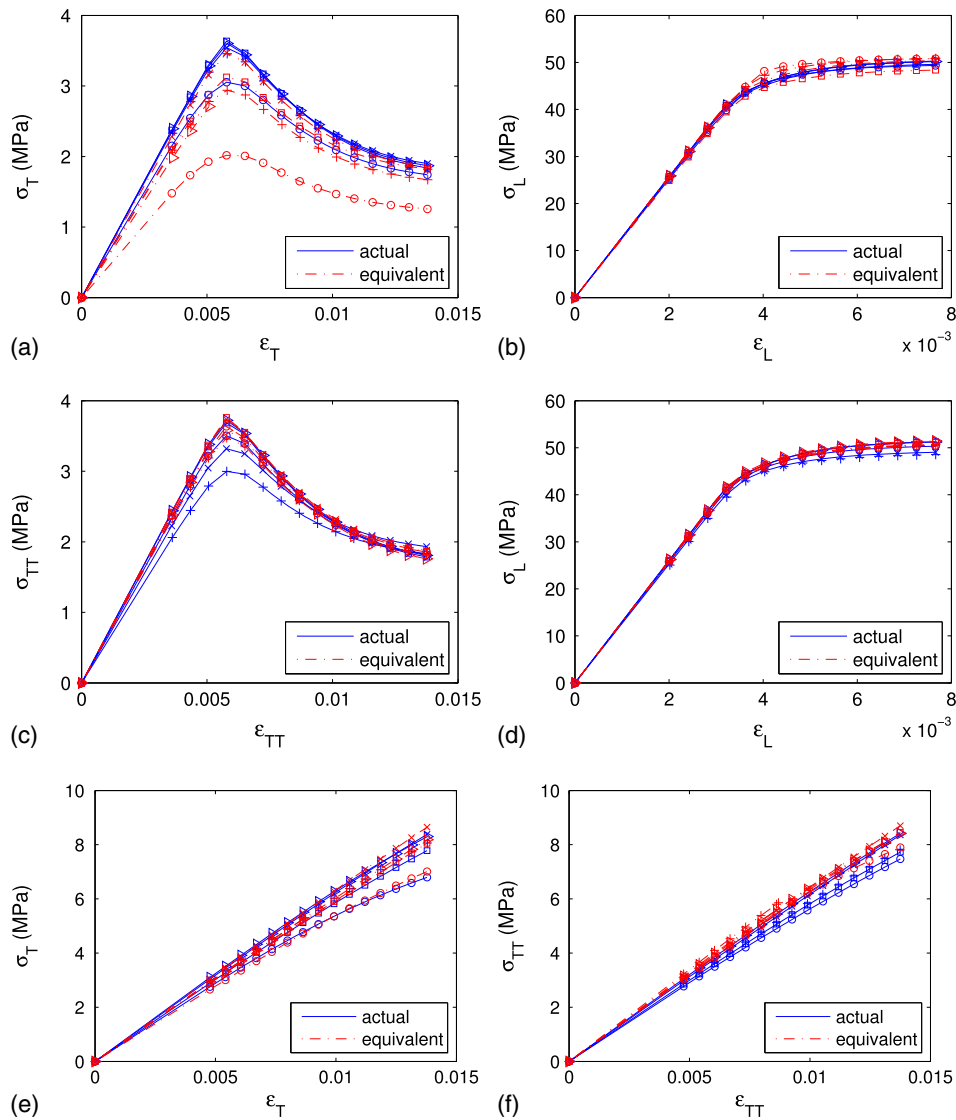


Fig. 6. Comparison of normal stresses along the directions of loading in the corresponding actual and equivalent models under biaxial compressive loading in each pair of material directions (σ_x : normal stress in x direction; ϵ_x : normal strain in x direction): (a) loading in T + L directions; (b) loading in T + L directions; (c) loading in TT + L directions; (d) loading in TT + L directions; (e) loading in T + TT directions; (f) loading in T + TT directions

Table 6. Mean and Standard Deviation of the Maximum Stresses of the Corresponding Actual and Equivalent Models Taken from the Same Position in the Parent Billet under Biaxial Compressive Loadings

Loading directions	T + TT		T + L		TT + L	
	Actual	Equivalent	Actual	Equivalent	Actual	Equivalent
Maximum stress 1						
Mean (MPa)	7.9	7.4	3.5	2.9	3.4	3.6
Standard deviation (MPa)	0.6	1.3	0.2	0.5	0.3	0.1
Maximum stress 2						
Mean (MPa)	8.0	7.9	49.9	47.3	50.1	50.9
Standard deviation (MPa)	0.4	1.2	0.4	6.3	1.2	0.4

$$f_{\text{yield}} = \frac{(\sigma_X - \sigma_Y)^2}{(6.2 \text{ MPa})^2} - 1 \quad (13)$$

But equal displacement steps and elastic moduli in loading directions result in

$$\Delta\sigma_X \approx \Delta\sigma_Y \Rightarrow \Delta(\sigma_X - \sigma_Y) < \Delta\sigma_X \quad (14)$$

Therefore, hardening is predictable in case of loading in T + TT directions because the change in $\Delta(\sigma_X - \sigma_Y)$ is very small.

Statistical Testing

Table 7 contains the p-values evaluated by the Student's T and Wilcoxon tests for the maximum stresses obtained from the simulations with biaxial loading scenarios. As expected, for the T + L

Table 7. P-Values of Student's T and Wilcoxon Tests under the Null Hypothesis H_{0p} Evaluated for the Biaxial Loading Scenarios

Loading directions	Maximum stress 1		Maximum stress 2	
	T-test	Wilcoxon test	T-test	Wilcoxon test
T + TT (%)	51.1	84.1	85.8	31.0
T + L (%)	2.3	5.6	42.8	69.1
TT + L (%)	19.1	31.0	15.1	42.1

loading, there is uncertainty if ellipsoids are good replacements for actual voids. When the maximum stresses along the T direction are considered, the Student's T test rejects the null hypothesis (H_{0p}) that the distributions are the same, while Wilcoxon test does not. Neither method rejects the null hypothesis when the maximum stresses along the L direction are taken into consideration. It is speculated that if more samples were considered with the Student's T test, like the Wilcoxon test, it would not reject the null hypothesis. The other possible reason why the Student's T test rejected the null hypothesis is that the distribution of $x_a - x_e$ is probably not a normal distribution. That is why more consistent results were obtained with the nonparametric Wilcoxon test.

In summary, (1) the ellipsoidal replacement acts sufficiently well under uniaxial loading in L direction; (2) a proper consistency is seen between actual and ellipsoidal models under biaxial loading; (3) with just one exception, the Student's T and Wilcoxon tests did not reject the null hypothesis; and that (4) the material strength in T direction (the most problematic direction) is so low that even 15% difference of strength estimation means less than 1 MPa difference. Our opinion is that ellipsoids are effective replacement shapes for actual voids in modeling PSL under compression.

Conclusions

The focus of this paper was on the linear and nonlinear compressive behavior of parallel strand lumber when actual voids are modeled by equivalent ellipsoids. The motivation for such replacement was to gain insight into the void shape effect on PSL mechanical behavior. In all simulations, the wood phase was assumed continuum and deterministic, while the void phase was the only source of uncertainty.

Linear analyses indicated that for all uniaxial loading scenarios, comparing corresponding models containing actual voids and

equivalent ellipsoids, the effective moduli of elasticity and the distributions of element stresses of different types matched acceptably. For ductile compressive behavior, when nonlinear uniaxial and biaxial compressive loading scenarios were studied, virtual ellipsoids were also found to be appropriate model representations for actual voids of PSL. The statistical study presented in the paper supports this conclusion.

References

- ADINA R&D. (2012). *ADINA structures—Theory and modeling guide, 3.4: Isothermal plasticity material models*, Watertown, MA.
- Amini, A. (2013). "Mesosstructural characterization and probabilistic modeling of the design limit states of parallel strand lumber." Ph.D. thesis, Univ. of Massachusetts at Amherst, Amherst, MA.
- Amini, A., Arwade, S. R., Clouston, P. L., and Rattanaserikiat, S. (2014). "Characterization and probabilistic modeling of the mesostructure of parallel strand lumber." *J. Mater. Civ. Eng.*, 10.1061/(ASCE)MT.1943-5533.0001116, 04014179.
- Arwade, S. R., Clouston, P. L., and Winans, R. (2009). "Measurement and computational modeling of the elastic properties of parallel strand lumber." *J. Eng. Mech.*, 10.1061/(ASCE)EM.1943-7889.0000020, 897–905.
- Arwade, S. R., Winans, R., and Clouston, P. L. (2010). "Variability of the compressive strength of parallel strand lumber." *J. Eng. Mech.*, 10.1061/(ASCE)EM.1943-7889.0000079, 405–412.
- Bejo, L., and Lang, E. M. (2004). "Simulation based modeling of the elastic properties of structural composite lumber." *Wood Fiber Sci.*, 36(3), 395–410.
- Clouston, P. L., and Lam, F. (2001). "Computational modeling of strand-based wood composites." *J. Eng. Mech.*, 10.1061/(ASCE)0733-9399(2001)127:8(844), 844–851.
- Forest Products Laboratory. (2010). "Wood handbook: Wood as an engineering material." *General Technical Rep. FPL-GTR-190*, U.S. Dept. of Agriculture, Forest Service, Forest Products Laboratory, Madison, WI, 508.
- Hibbeler, R. C. (2011). *Mechanics of materials. 3.3: Stress-strain behavior of ductile and brittle materials*, 8th Ed., Prentice Hall, Upper Saddle River, NJ.
- Janowiak, J. J., Hindman, D. P., and Manbeck, H. B. (2000). "Orthotropic behavior of lumber composite materials." *Wood Fiber Sci.*, 33(4), 580–594.
- Jones, R. M. (1975). *Mechanics of composite materials*, Scripta Book Co., Washington, DC.
- Mc Clave, J. T. (2012). *Statistics*, 12th Ed., Pearson, London.